

# BDX on-beam background assess and MC validation

M. Battaglieri, A. Celentano, R. De Vita, L. Marsicano  
*Istituto Nazionale di Fisica Nucleare, Sezione di Genova, 16146 Genova, Italy*

M. Bondi, M. De Napoli, N. Randazzo  
*Istituto Nazionale di Fisica Nucleare, Sezione di Catania, Catania, Italy*

G. Kharashvili, E.S. Smith  
*Jefferson Lab, Newport News, VA 23606, USA*

E. Izaguirre  
*Perimeter Institute for Theoretical Physics, Waterloo, Ontario, Canada, N2L 2Y5*

G. Krnjaic  
*Center for Particle Astrophysics, Fermi National Accelerator Laboratory, Batavia, IL 60510*

D. Snowden-Ifft  
*Occidental College, Los Angeles, California 90041, USA*

M. Carpinelli, V. Sipala  
*Università di Sassari e Istituto Nazionale di Fisica Nucleare, 07100 Sassari, Italy*

*and The BDX Collaboration*

## Abstract

In response to the issue raised by JLAB-PAC44 about the experiment proposal *PR-16-001 Dark matter search in a Beam-Dump eXperiment (BDX) at Jefferson Lab* [?] we propose to measure the muon flux and the prompt background produced by the interaction of the high intensity 11 GeV electron beam with the Hall-A beam-dump. The muon flux will be sampled at different height (with-respect-to the beam axes), positions and angles downstream of the beam-dump to map-out the radiation field in the location of the future BDX hall. In order to realistically assess the beam-on background experienced by the BDX detector, a specimen of the CsI(Tl) crystal used in the BDX electromagnetic calorimeter, will be exposed to the radiation as component of a plastic scintillator hodoscope built specifically for this measurement (BDX-Hodo). The use of a loose trigger will provide further information on beam-related low energy background (dominated by neutrons). Although it will not be possible to directly compare results of this test with the experimental set-up proposed in PR-16-001, that will make use of a different and optimised shielding, the measurement will be extremely useful to validate the MonteCarlo simulation tools (GEANT4 and FLUKA) used to design the new underground facility and optimize the BDX detector.

This report is organised as follow: results of the simulation of the radiation field produced by the interaction of the beam with the dump are reported in Sec. ??; the experimental set-up and the detector is described in Sec.??; the expected results of the measurement are reported in Sec. ?. Details about cost estimate, work- and time-planes are reported in the Appendix.

## Contents

DRAFT

# 1 MC simulations

## 1.1 The Hall-A high-power beam-dump

The Hall A and C use identical high-power absorbing (up to 1 MW) beam-dumps to stop the 11 GeV beam, remnant of beam/target interaction. The dump is made by a set of about 80 aluminium disks, each approximately 40 cm in diameter of increasing thickness (from 1 to 2 cm), for a total length of approximately 200 cm, followed by a solid Al cylinder 50 cm in diameter and approximately 100 cm long. They are both cooled by circulating water. The full drawing of the beam-dump is shown in Fig. ???. To increase the radiation shielding, the thickness of the concrete tunnel surrounding the Al dump is about 4-5 m thick.

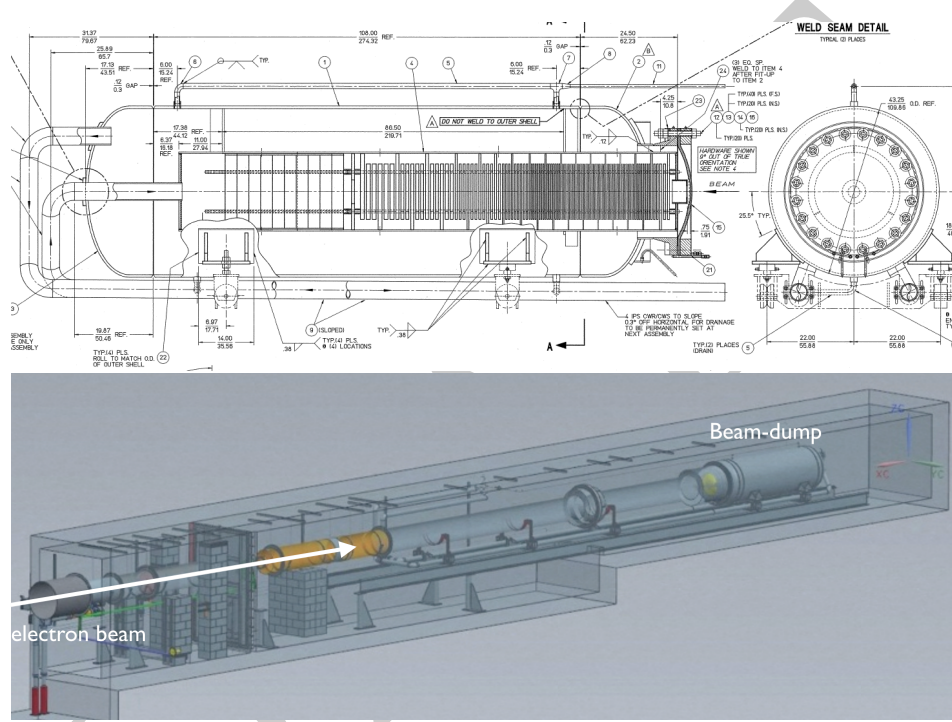


Figure 1: Hall-A beam dump and beam dump enclosure.

## 1.2 The beam-dump model in FLUKA

The beam-dump geometry and materials have been implemented in FLUKA-2011.2c.5 by the Jefferson Lab Radiation Control Department. Details are reported in Ref. [?]. The input card used to run the program includes all physics processes and a tuned set of weight biasing to speed up the running time while preserving the results accuracy. The  $\mu$ , n, and  $\gamma$  fluence (differential in angle and energy) per EOT were calculated at XXX cm downstream of the beam-dump exit, through a circular area of 105 cm<sup>2</sup>. Figure ?? shows the FLUKA graphic representation of the beam-dump and the location of the flux detector. In our model we extended the original beam-dump description, by including the proper geometry and material composition around and downstream of the beam-dump. Figure ??



Figure 2: Hall-A beam-dump implementation in FLUKA.

shows the geometry of the concrete bunker surrounding the beam-dump and the downstream area filled by soil as implemented in our FLUKA model.

### 1.3 The beam-dump model in GEANT4 (GEMC)

The beam-dump, as well as the geometry and composition of surrounding environment, has been implemented in GEANT4 using the GEMC tool [?]. This model is a refined version with-respect-to the one used in PR-16-001 [?] that better describes the beam-dump geometry, matching the level of details implemented in the FLUKA model. For a better description of muon transportation, the `G4GammaConversionToMuons` has been added to the standard physics list used in simulations of PR-16-001(`FTFP_BERT_HP + STD + HP`). Particles fluence has been sampled by mean of a flux detector positioned in the same location as in the FLUKA model. Figure ?? shows the beam-dump and vicinity implemented in GEMC.

### 1.4 Muons from beam-dump interaction

A comparison of muon fluence downstream of the beam-dump (see above for details about the location) obtained by FLUKA and GEMC are reported in Fig. ???. Considering that low energy muons are absorbed by the bunker-head shielding, to keep the GEMC running time reasonable, only

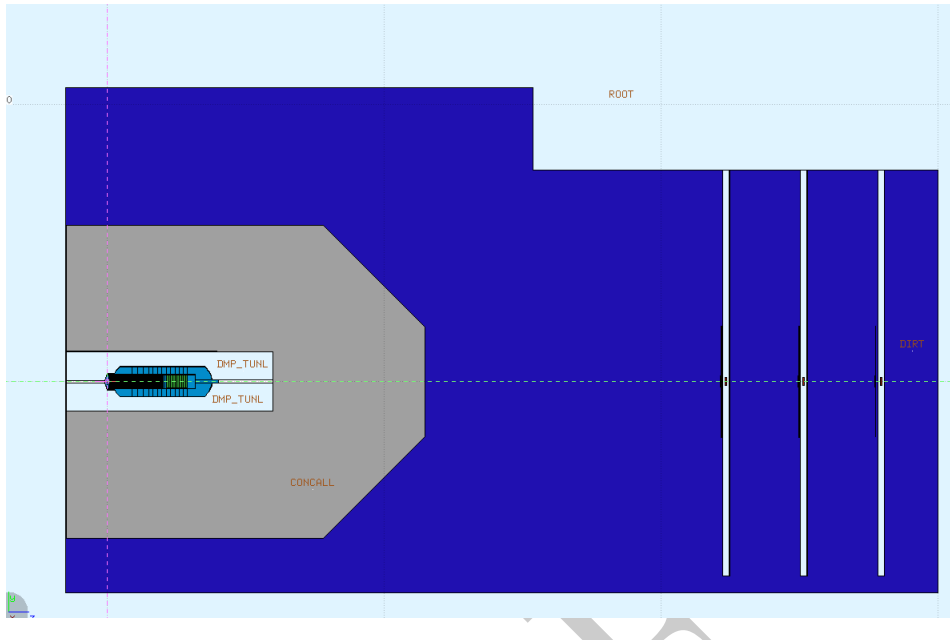


Figure 3: The geometry/composition of the concrete bunker surrounding the beam-dump and the downstream soil as implemented in FLUKA.

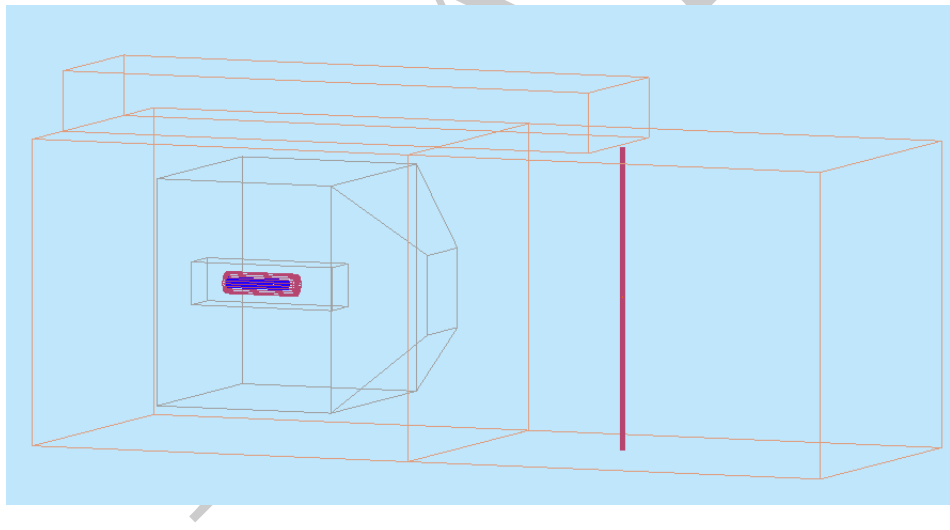


Figure 4: The geometry/composition of the beam-dump, the sourraunding concrete bunker and the soil as implemented in GEMC. The drawings also shows the pipe used to lower the BDX-Hodo detector at the beam-line depth.

particles with energy grater than 100 MeV (`ENERGY_CUT=100*MeV`) has been tracked and sampled. A total of  $4 \times 10^9$  ( $9 \times 10^6$ ) EOT have been simulated with GEMC (FLUKA). The comparison of the two simulations shows a perfect agreement in the full energy range where data were generated.

In spite of a factor of  $\times 100$  less statistics, FLUKA shows, as expected, smaller error bars. This reflects the optimised weight biasing used by the simulation to generate high statistics for the low probability processes keeping the total number of events limited. To penetrate the concrete shielding and the soil, a minimum energy of  $E_\mu > 4$  GeV is required. With this energy cut, the integrated number of muon per EOT results in  $4.8 \pm 0.1 \times 10^{-7}$  ( $5.5 \pm 0.2 \times 10^{-7}$ ) for GEMC and FLUKA respectively. Figure ?? shows the correlation between the muon energy and the azimuthal angle (with-respect-to the beam axes): the regions populated in both simulations show a similar shape.

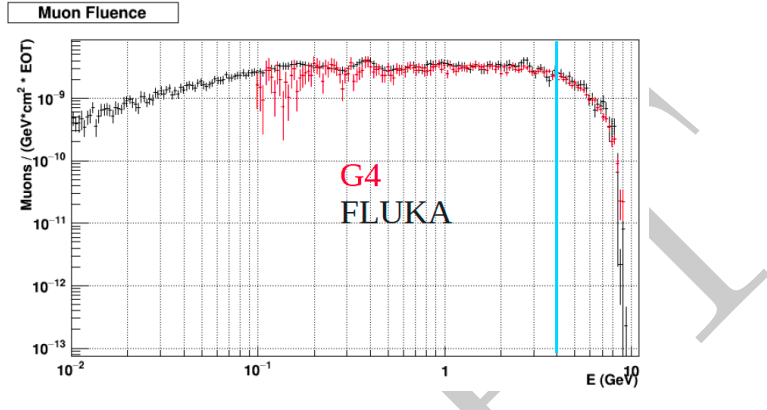


Figure 5: Muon fluence downstream of the beam-dump obtained by FLUKA (black) and GEMC (red). The GEMC simulations started at  $E_\mu = 100$  MeV.

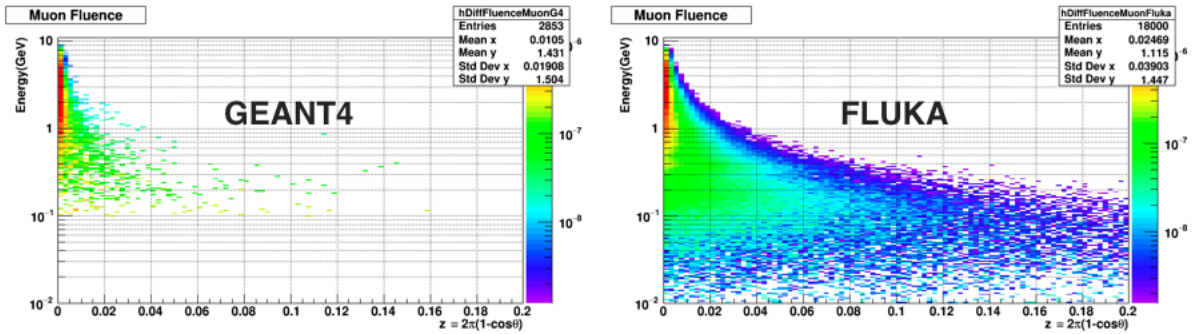


Figure 6: Energy vs. azimuthal angle of muons crossing the flux detector located downstream of the beam-dump obtained by FLUKA and GEMC.

## 1.5 Sampling and particle transport

The good agreement between two independent simulation tools (FLUKA and GEMC) gives us confidence about reliability of the obtained results. Both methods have pros and cons. FLUKA shows a superior speed in running but a complicated implementation of variables of interest (e.g. the final output is given via *scores* such as fluence or distribution in specific locations need to be pre-defined). GEMC (GEANT4) tracks particles in all volumes providing a straightforward output

(particle four-momenta) in the desired flux detector but requires an un-practical running time to collect a reasonable statistics (in particular when an em shower is involved). In the following we describe how we overtook these difficulties.

### 1.5.1 Muons - GEMC

We used GEMC to simulate muons. To make the process more efficient, we followed the procedure described below:

- we used a low statistic sample of EOT to simulate the interaction of the 11 GeV electrons with the beam-dump;
- we sampled the muon flux and variables (momentum, azimuthal angle and transverse position) on a flux detector located downstream of the beam-dump;
- we used distributions obtained in the previous step as input of a custom event-generator to produce a high statistic muon sample;
- we used GEMC to transport muons downstream of the beam-dump all the way down to the desired location(s) of BDX-Hodo;
- we implemented the BDX-Hodo response in GEMC to realistically describe the muon detection.

The area where muons are sampled from the primary beam/dump interaction and used as source in the custom-made event generator is shown in Fig. ??.

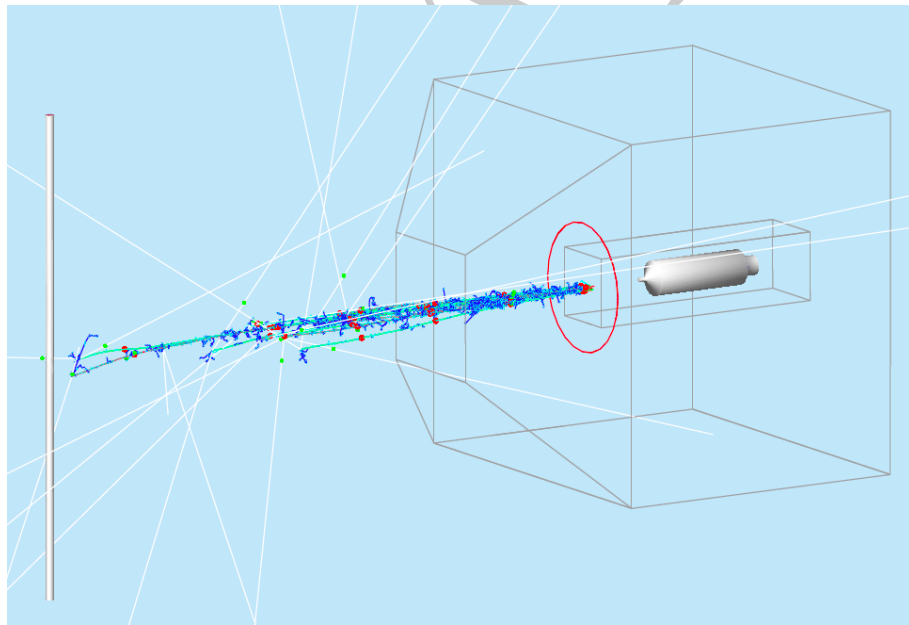


Figure 7: The  $\mu$  sampling/generation area is the surface surrounded by the magenta circle.

Figure ?? shows the muon distributions (energy vs azimuthal angle and radial distance from the beam line) downstream of the beam-dump, as obtained by the full GEMC simulation of 11

GeV electrons hitting the beam-dump. The left panel of Fig. ?? shows the distributions obtained by running the full simulation with GEMC compared to the custom event generator results. As a check, the right panel of the same figure shows the comparison in the location of interest ( $\sim 20$  m downstream of the beam-dump). The difference in the error bar size indicates the improvement obtained by adopting this procedure.

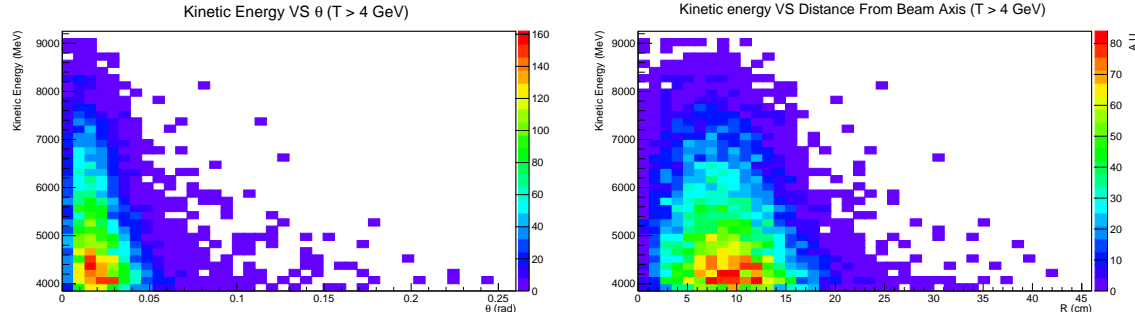


Figure 8: Muon kinetic energy vs. azimuthal angle (left) and distance (right) from the beam-line axes as obtained by the full GEMC simulation.

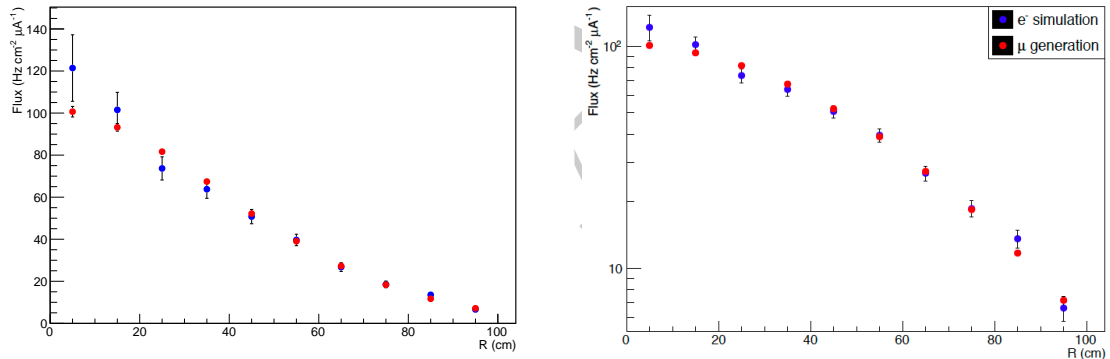


Figure 9: Muon flux as a function of the radial distance from the beam axes obtained by GEMC (blue) and by the custom event-generator (red) at the sampling/generation location (left) and in the region of interest (right),  $\sim 20$  m downstream of the beam-dump.

### 1.5.2 Background - FLUKA

We used FLUKA to estimate the background expected in the BDX-Hodo detector. We simulated an 11 GeV electron-beam interacting with the beam-dump, propagate all particles to the location of interest obtaining the fluence on the CsI(Tl) surface. Figure ?? shows the resulting fluence per EOT as a function of energy for all particles (black) and muons only (red). As expected, muons are the only high energetic particles reaching the crystal while other species (neutrons mainly) account for the low energy of the spectrum. More details are reported in Sec. ??.

### Impinging particles

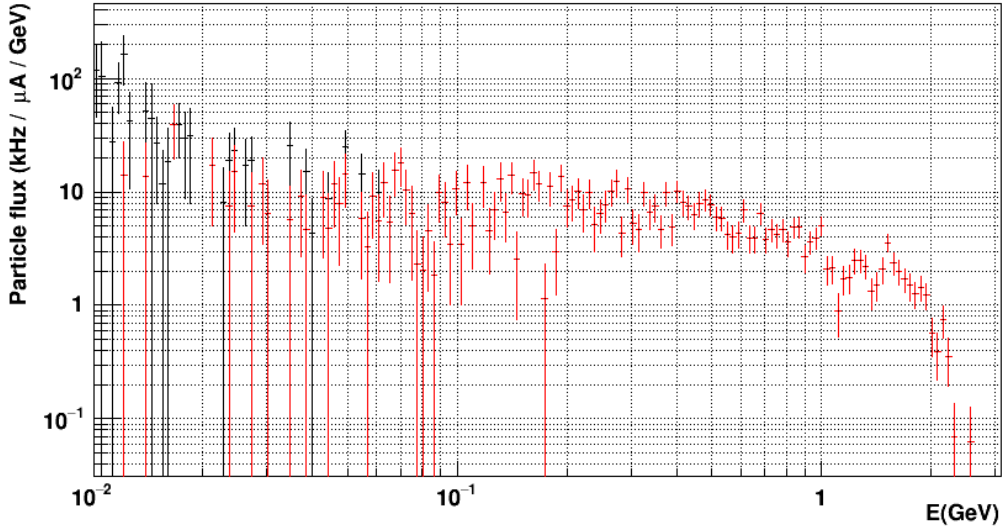


Figure 10: Fluence on CsI(Tl) crystal of all crossing particles (black) and muons only (red). The crystal is located in the region of interest  $\sim 20$  m downstream of the beam-dump.

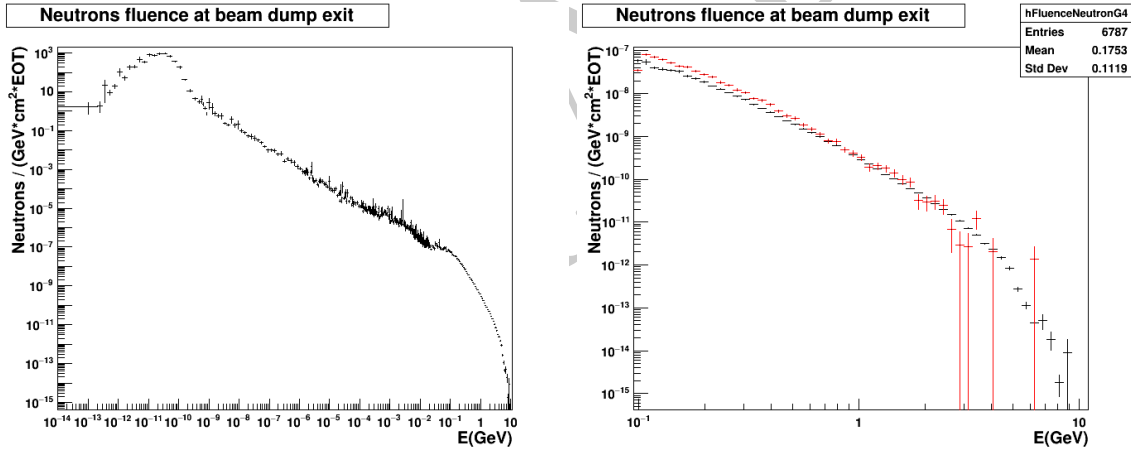


Figure 11: Neutron spectrum downstream of the the dump obtained by full FLUKA simulation (left). The right panel shows the comparison between FLUKA (black) and GEMC (red) for the high energy part pf the spectrum.

It's interesting to note that the spectrum of high energy neutrons ,  $T_n > 100$  MeV, (sampled downstream of the dump) obtained by GEMC is in good agreement with FLUKA (see Fig. ??). The agreement indicates that, in this energy range, both simulation tools are reliable.

Another interesting aspect of the neutron spectrum is shown in Fig. ?? . The energy spectrum (sampled downstream of the dump) obtained by FLUKA by RadCon (Ref. [?]) is compared to the same plot obtained by our FLUKA simulations. The two models differ in the implementation of

the beam-dump vault: a detailed description of the material surrounding the dump, that includes air and concrete, versus a simplified geometry/material description. The effect is clearly visible in the low energy part of the spectrum (while the high energy part is almost identical) proving that a detailed description of the dump enclosure is necessary to correctly describe the low energy backgrounds.

Figure 12: Neutron differential fluence downstream of HPBD

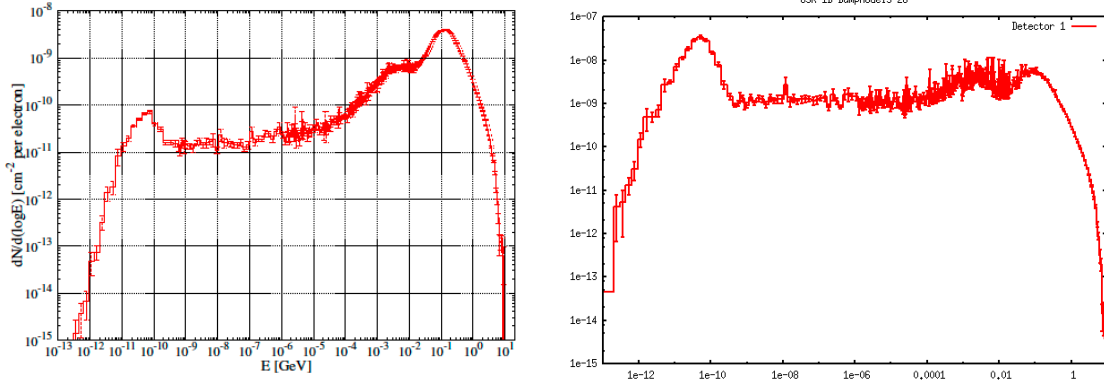


Figure 12: Comparison of neutron energy spectrum obtained by FLUKA, sampled downstream of the beam-dump with a simplified geometry (left) and including vault surrounding materials (right). The number of low energy neutrons significantly increases when the reflection on the wall is considered.

Muon and background flux at the location of interest will be discussed in details in the Sec. ?? after presenting the BDX-Hodo detector in the next Section.

## 2 Test set-up



Hall A Beam Dump / C1

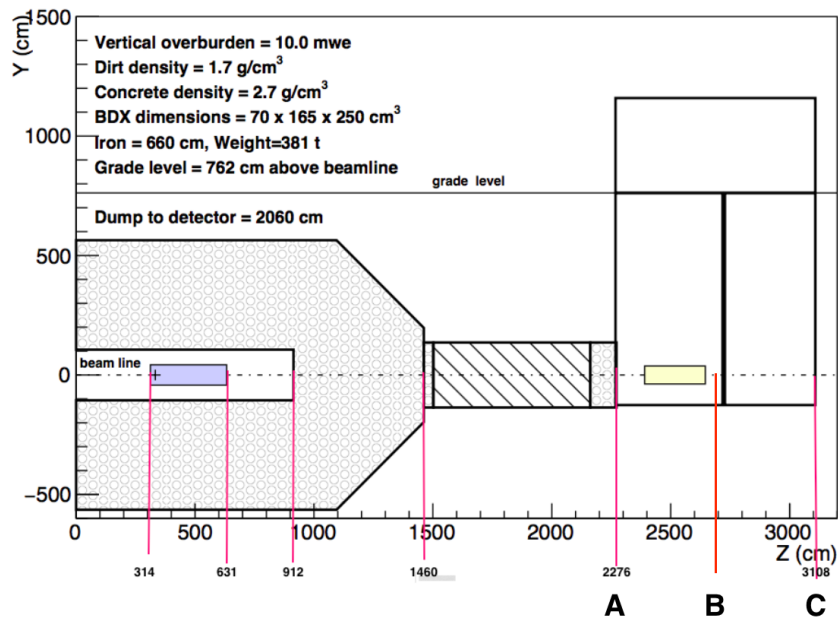


Figure 13: The area downstream of the Hall-A beam-dump and the studied test locations.

### 2.1 Detector location

The area downstream of Hall-A beam-dump is shown in Fig. ?? together with the corresponding location with-respect-to the new underground facility proposed in PR-16-001 [?]. The three posi-

tions, indicated with markers **A**, **B** and **C**, correspond to the hall entrance (22.4 m downstream of the beam-dump entrance), a point in the middle (25.2 m) and the exit (28 m), respectively. The experimental set-up we are proposing assumes to dig a well and insert a pipe in one (or more) of these locations. The BDX-Hodo detector will be lowered in the pipe and muon flux sampled at different height wrt. the beam-line nominal height. The muon flux profiles in Y (vertical direction), measured in different location in Z (distance from the dump), will allow us to compare the absolute and relative MC predictions.

## 2.2 The BDX-Hodo detector

The detector used to measure the beam-on-related muon radiation and the background in the proximity of the new BDX underground facility will make use of a BDX ECal CsI(Tl) crystal sandwiched between a set of segmented plastic scintillators. A CAD representation as well as a vertical and horizontal cut with dimensions are shown in Fig. ???. The front of the crystal will be equipped with two

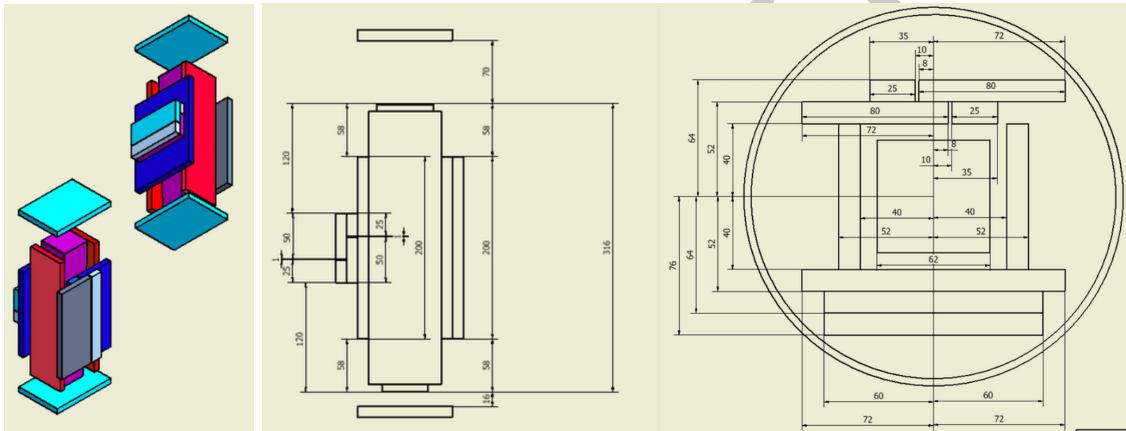


Figure 14: The CAD representation of the BDX-Hodo detector and some drawings with geometry and sizes.

layers of plastic scintillators, each composed by a large and a small 1 cm-thick scintillators strips. The overlap of the four paddles (each 20 cm long in Y) results in three independent 2.5 cm channels along the X (horizontal) direction. The same concept was applied to the back side of the crystal but with paddles tilted by 90 degrees to define three 2.5 cm independent channels along the Y (vertical) direction. The requirement of a hit in both front and back paddles defines a 3x3 matrix of  $2.5 \times 2.5 \text{ cm}^2$  pixels providing a cm-like muon XY position resolution. The addition of a larger paddle ( $20 \times 14.4 \text{ cm}^2$ ) on the back provides an enhanced sensitivity in the unlikely case rates will be much lower than what estimated by MC simulations. Four more paddles covering the left/right sides and the top/bottom of the crystal will be used to veto cosmic rays and other radiation not associated to the beam direction. The crystals will be coupled, on the large side, to a  $6 \times 6 \text{ mm}^2$  Hamamatsu S13360-6025 SiPM as described in Sec. 3.2.1 of PR-16-001 [?]. The scintillator paddles will be made with extruded plastic, each read out via a WLS fiber coupled to a  $3 \times 3 \text{ mm}^2$  Hamamatsu S12572-100 SiPM sharing the same technology used in the BDX Inner Veto detector (described in details in Sec. 3.2.2 of PR-16-001). Muons produced by the electron beam will be detected by requiring a 5-fold coincidence (two front paddles + CsI(Tl) crystal + two back paddles). The detector will be contained in a 20-cm diameter stainless-steel cylindrical vessel, covered on top and on the bottom

by steel lids. The whole assembly will be water-tight to prevent any water leak inside the vessel. A stainless-steel extension on the top cover will be used to run cables (signal and power) from the detector to the ground-level. The extension, made by a 1-inch stainless steel pipe, rigidly attached to the whole assembly, will be also used to remotely control the cylinder orientation providing correct the alignment of the BDX-Hodo wrt. the beam axes.

To record the 13 (scintillators) + 1 (crystal) channels single 16ch fADC board and a VME crate will suffice. The full DAQ system (crate + pc) will be shielded in a van parked close to the well entrance. The power will be provided by a diesel power generator to minimize the requirements of long extension cords.

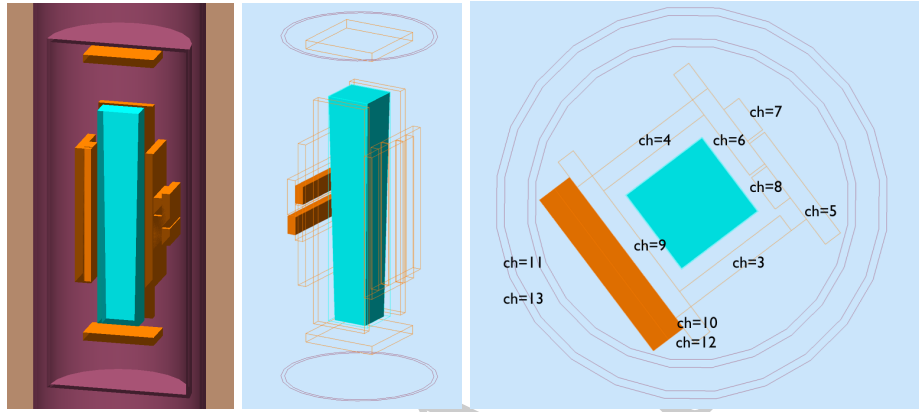


Figure 15: The GEMC implementation of the BDX-Hodo detector.

The detector geometry as well as the realistic response of the CsI(Tl) crystal and plastic scintillators have been implemented in GEMC (see Appendix B.2 of PR-16-001 [?] for details about the detectors response parametrisation). Figure ?? shows the BDX-Hodo implementation in GEMC. To estimate rates, we assumed a detection threshold of 10 phe in scintillators and 100 phe in the crystal corresponding to 400 keV and 2 MeV of deposited energy respectively\*.

---

\*MIPs release  $\sim 50$  phe ( $\sim 2$  MeV) and  $1670$  phe ( $\sim 32$  MeV) respectively.

### 3 Results

Muons and beam-related background were generated by the 11 GeV electron beam interaction with the beam-dump and propagated in the region of interest as described in Sec. ??.

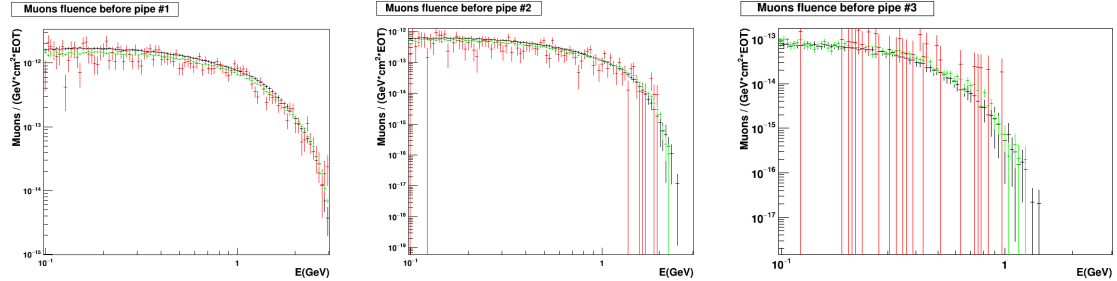


Figure 16: Muons differential fluence at the three locations of interest (A, B and C). Beam/dump interaction using FLUKA (black), GEMC (red) and the high statistic custom  $\mu$  event generator with GEMC propagation (green).

#### 3.1 Muon detection

Fig. ?? shows the muon flux crossing the BDX-Hodo as obtained by GEMC and FLUKA in the three locations of interest (**A**, **B** and **C**). The flux has been sampled assuming the BDX-Hodo centered to the beam-line depth. Results are reported for muons generated at high statistic by the custom  $\mu$  event generator and propagated using GEMC (green points in the figure). The number of event generated at the dump correspond to  $(1.2 \pm 0.1) 10^{12}$  EOT or one second of  $0.2 \mu\text{A}$  current. Rates in crystal, scintillators and requiring a 5-fold coincidence of the two front/back layers of plastic with the crystal are reported in Tab. ?? for a beam current of  $10 \mu\text{A}$  and detection thresholds as listed in the previous Section. Results show a drop in rate by about one order of magnitude when moving from one location to the next. Table ?? shows the expected rate measured in position **C** when the BDX-Hodo detector is off-axes by  $40/80$  cm. The measurement of muon rate at different heights (angles) wrt to the beam-line (beam-dump) will provide further information to validate simulations. Fluxes in position **C** (or/and **B**) are large enough to be detectable (significantly higher than cosmic muons and beam-dump neutron background) and manageable by crystal, SiPms and front-end electronics (no pile-up effects expected). These two locations are close to the paved road and easily accessible by the drilling machine and related equipment. Similar conclusions (scaling rates by 10) hold if the beam current drops/increases by one order of magnitude ( $1/100 \mu\text{A}$ ) making the test feasible in parallel to any 11 GeV operation of Hall-A.

#### 3.2 Muon flux above-the-ground

For sake of completeness the muon flux has also been evaluated by using FLUKA in the closest locations accessible above the beam-dump vault . This set-up assumes to locate the detector above-the-ground with no drilling required largely simplifying the test. Due to the CPU-time necessary to track muons at such large angle (with respect to the beam axis) we used a two steps procedure. Firstly, the 11 GeV electron beam was let to interact with the beam-dump and muons produced on the roof of the vault sampled in four different locations (shown in Fig. ??-left ). A high statistic sample of muons have then been generated according to the previous distributions and propagated

Table 1: Beam-on muon rates expected in BDX-Hodo for  $I_{beam}=10\mu A$  in locations **A**, **B**, and **C**.

Location	Rate <sub>Crystal</sub> (kHz)	Rate <sub>Front-Back Scint</sub> (kHz)	Rate <sub>Coin</sub> (kHz)	Rate <sub>XY ch</sub> (kHz)
<b>A</b>	120	120/40	24	4.5
<b>B</b>	20	22/8	3.7	0.7
<b>C</b>	2.8	2.5/1	0.5	0.1

Table 2: Beam-on muon rates expected in BDX-Hodo for  $I_{beam}=10\mu A$  in position **C** sampled at different vertical distance from the beam-line.

Vertical distance	Rate <sub>Crystal</sub> (kHz)	Rate <sub>Front-Back Scint</sub> (kHz)	Rate <sub>Coin</sub> (kHz)	Rate <sub>XY ch</sub> (kHz)
0 (nominal)	2.8	2.5/1	0.5	0.1
40 cm	1.4	2.5/1.5	0.17	0.04
80 cm	0.6	0.6/0.3	0.08	0.02

to the outside. Applying a conservative hypothesis (the muons are propagated perpendicular to the beam axis crossing the minimal amount of concrete and dirt) muons with energy higher than 4.5 GeV (the minimum to not been ranged out) were propagated and sampled in the four perpendicular outdoor positions. Figure ??-right shows the four locations ( $A_{Ext}$ ,  $B_{Ext}$ ,  $C_{Ext}$ , and  $D_{Ext}$ ) on top of the hill. Integrating over the surface of the BDX-Hodo detector ( $\sim 100 \text{ cm}^2$ ) and considering as a reference a beam current of  $10 \mu A$ , no sizeable muon flux would be detected (Rate<sub>Max</sub> < 3 Hz). Rates in the different outdoor locations are listed in Tab. ??.

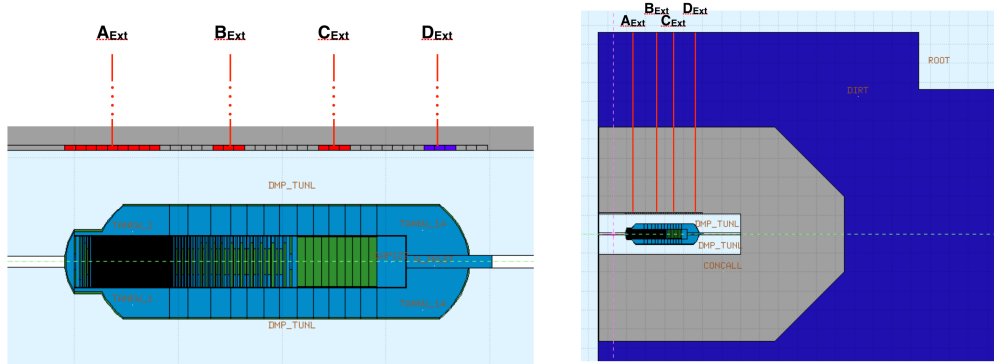


Figure 17: Left: In red are shown the points on the roof where muon flux has been sampled. Right:  $A_{Ext}$ ,  $B_{Ext}$ ,  $C_{Ext}$ , and  $D_{Ext}$  are the four location outdoor where the muon flux has been evaluated.

Table 3: Beam-on muon rate expected outdoor, on top of the beam-dump hill.

Location	Rate <sub>Crystral</sub> (Hz / (cm <sup>2</sup> μA))
A <sub>Ext</sub>	2.2 10 <sup>-3</sup>
B <sub>Ext</sub>	4.7 10 <sup>-4</sup>
C <sub>Ext</sub>	1.9 10 <sup>-3</sup>
D <sub>Ext</sub>	negligible

### 3.2.1 Beam-related background

Beside muons, other particles are produced in the 11 GeV electron beam interaction with the dump. The majority (electrons, gamma, nuclei and fragments) are ranged-out well before to reach the region of interest but some (low energy neutrons, mainly) may propagate through concrete and dirt reaching the BDX-Hodo detector. Fig. ?? shows the neutron flux in the three locations of interest as obtained by FLUKA simulations.

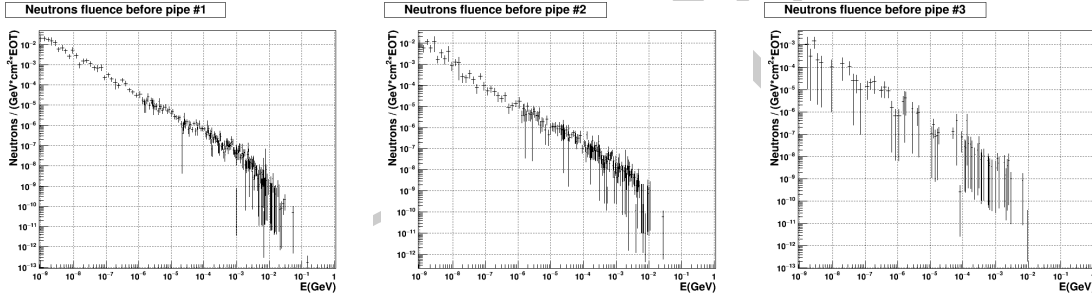


Figure 18: Neutron differential fluence at the three locations of interest. Spectra are obtained from electron beam interaction with the beam-dump using FLUKA.

For a complete understanding of the low energy (< MeV) background in the BDX-Hodo crystal, particles produced in the dump can not be tracked separately since some of them are produced along the way (e.g. by energetic muons or neutrons in the proximity of the detector). On top of that, neutral particles (in particular low energy/thermal neutron) do not directly interact with the crystal but deposit a visible energy via secondary interactions (e.g. gamma from nuclear capture in the surrounding material) making hard, if not impossible, to track back the background source. For all the above mentioned reasons we evaluated the background by running the full FLUKA simulation of 11 GeV electrons interaction with the beam-dump recording the deposited energy in BDX-Hodo crystal. Figure ?? shows the fluence of all particles (black) and muons only (red) on the CsI(Tl) surface. As already noticed, the high energy range of the spectrum is saturated by muons. Figure ?? shows the deposited energy in the CsI(Tl) crystal (located in the three position of interest). Muons (shown in red) almost saturate the highest energies (the MIP peak is clearly visible around  $E_{Dep} = 32$  MeV) while the contribution from other particles (neutrons) accumulates at low energies.

The crystal integrated rate is reported in Fig. ?? as a function of the deposited energy (and detected photoelectrons). Considering that the experiment only records events with a deposited

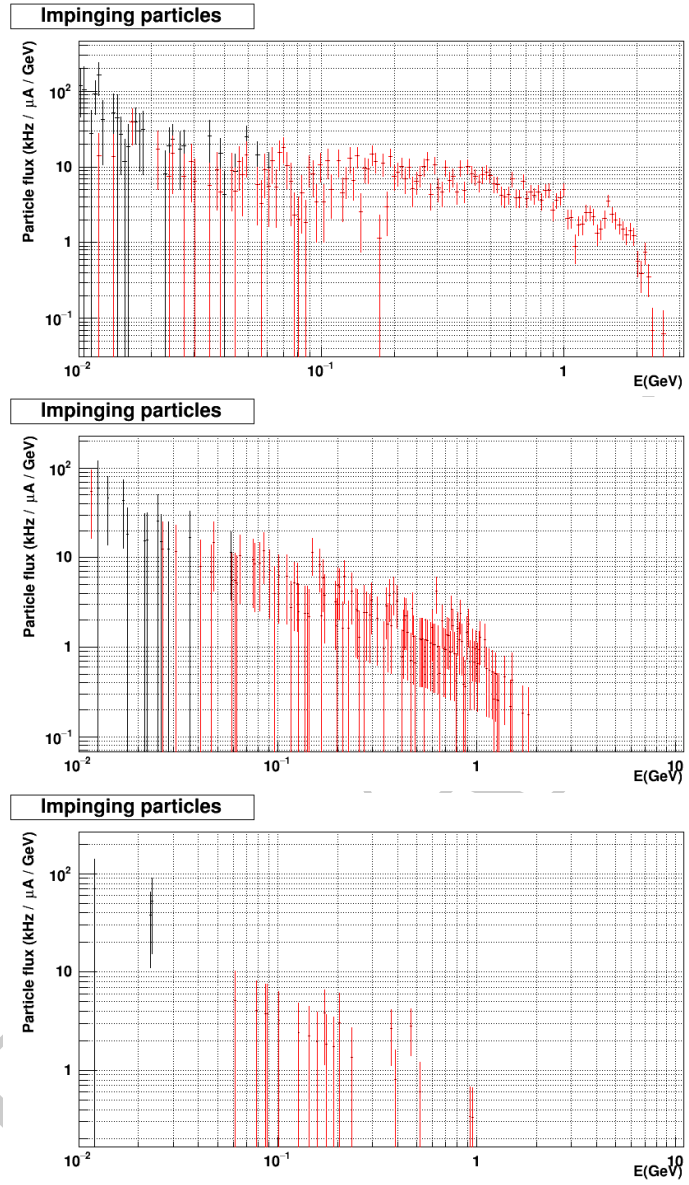


Figure 19: Fluence of all particles (black) and muons only (red) hitting the CsI(Tl) crystal. Plots refer to the crystal located in **A** (top), **B** (middle), and **C** (bottom).

energy in the crystal larger than 1 MeV (25 pe), the expected rate is in the range of 10 kHz.

### 3.2.2 Cosmic background

The cosmic muon background in the BDX-Hodo has been evaluated using GEMC. This is the same cosmic flux generator used in PR-16-001 [?]. The muon energy spectrum has been divided in

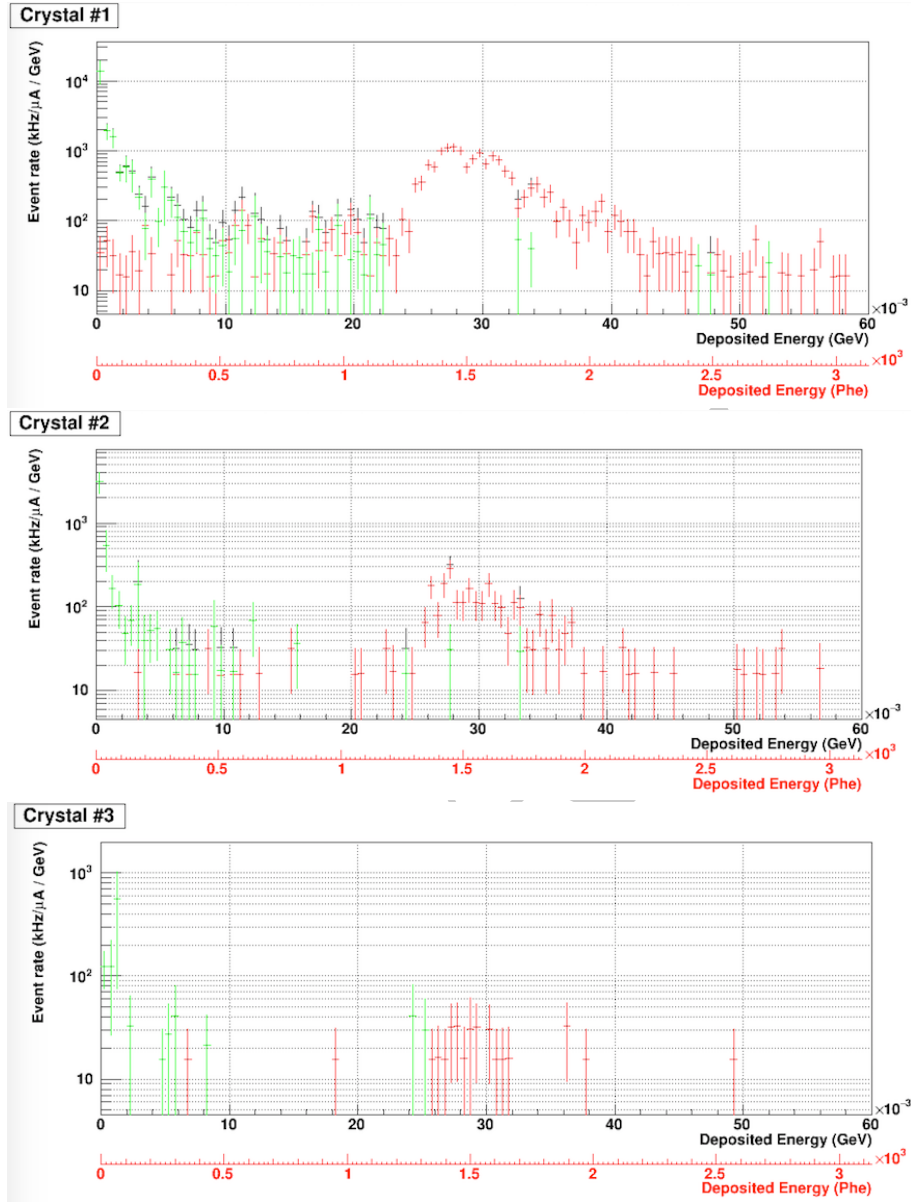


Figure 20: Distribution of energy deposited in the CsI(Tl) crystal by all particles (black), muons only (red) and the rest (green). The three plots refer to the crystal located in **A** (left), **B** (center), and **C** (right).

different ranges and correctly weighted to estimate the full rate expected on the detector. Rates have been evaluated for CsI(Tl) crystal, Top scintillator, and for the coincidence of the front/back scintillator with the crystal to mimic the condition used to identify and account for beam-on muons. We assumed the same detection thresholds used in the other rate estimates (10 phe and 100 phe for scintillators and crystal respectively). Tab. ?? shows the results of this study. The cosmic rate

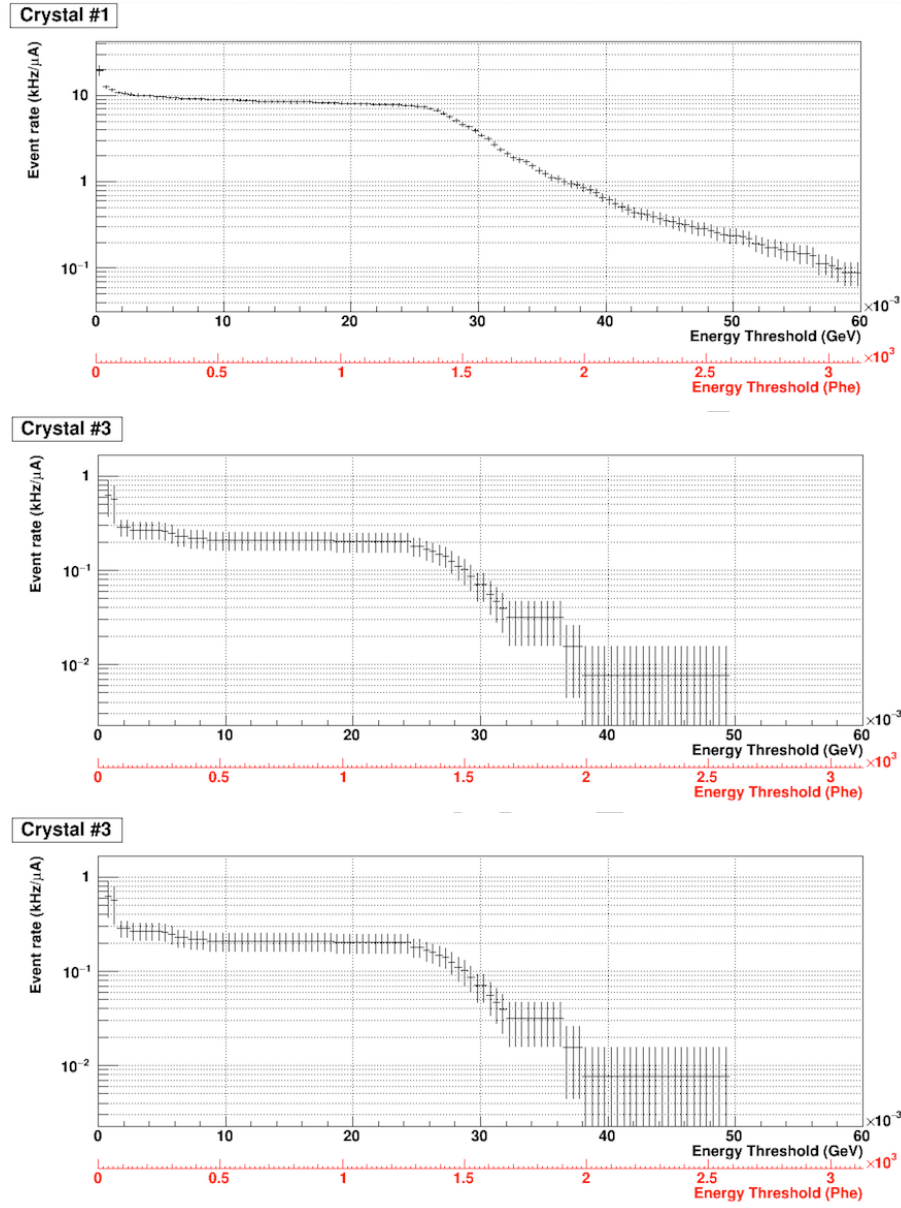


Figure 21: Crystal integrated rate as function of deposited energy. Plots refer to the crystal located in **A** (left), **B** (center), and **C** (right).

is negligible (in every condition  $< 1$  Hz) well below the expected rate of muons from the electron beam / beam-dump interaction.

Table 4: Cosmic rate expected in different components of BDX-Hodo

Energy range (GeV)	Rate <sub>Crystal</sub> (Hz)	Rate <sub>Top Scintillator</sub> (Hz)	Rate <sub>Coincidence</sub> (Hz)
0.2 - 2	0.01	0.02	0
2 - 10	0.2	0.25	0.01
10 - 100	0.35	0.4	0.01
Cosmic muon rate	0.56	0.67	0.02

### 3.3 Test configuration and practical details

Practical details (drilling technology, costs and schedule) and a work plan for the proposed test configuration are reported in the Appendix.

### 3.4 Summary

We simulated the interaction of a 11 GeV electron beam with the Hall-A beam-dump studying the radiation field in the beam-dump vault and  $\sim$ 20 m downstream in the area of the new underground facility required by the BDX experiment. Two different simulation tools (GEMC and FLUKA) were used. For some locations, results were compared with JLab Radiological Control Group estimates. Here are the main outcome:

- our results are consistent with what obtained by RadCon;
- we confirm that only (high energy) muons and (mainly thermal/low energy) neutrons propagates trough the beam-dump vault concrete walls and dirt reaching the region of interest;
- no sizeable flux was found outdoor in the closest locations above-the-ground;
- for energy greater than 100 MeV muon and neutron flux estimated with FLUKA and GEMC well match;
- for energy lower than 100 MeV FLUKA (using the biasing technique) resulted more efficient in run-time.

To validate MC tools and gain confidence in the beam-on background shielding optimization for the BDX experiment we propose to measure the muon flux in the region where the new underground facility will be located. Here below is the proposed experimental set up and the expected results:

- muons produced in the dump can be accessed by placing a detector downstream at the beam-line depth;
- a detector (BDX-Hodo) based on one CsI(Tl) crystal from BDX ECal, sandwiched between layers of scintillator counters will be specifically built for this measurement;
- two wells equipped by 10' pipes will be drilled 25.2 m and 28 m downstream of the beam-dump and the BDX-Hodo detector lowered in a pipe to cross the beam axes;

- rates of beam-on muons measured by BDX-Hodo are expected to be sizeable for a beam current of  $10 \mu A$  ( $\sim 3$  kHz and  $\sim 20$  kHz in the two locations respectively);
- given the count rates reported above, this measurement could be done with a variety of beam current ( $1 - 100 \mu A$ ) making the test fully parasitic wrt the Hall-A plans;
- this measurement was found to be insensitive to the cosmic muon background and other backgrounds (mainly) neutrons generated in the dump;
- the use of a BDX CsI(Tl) crystal will allow to prove the proposed technology in a background-rich environment worst than what expected in the BDX experiment<sup>†</sup>;
- once the pipes will be installed, tests will run for about a week, parasitically to any 11 GeV  $1-100 \mu A$ , Hall-A run; This test, measuring the muon flux (absolute and relative) in different location in Z (distance from the dump) and Y (vertical) will address the concern expressed by PAC44 report about the beam-on background in the BDX experiment.

---

<sup>†</sup>The BDX experiment foresees an optimised shilding that will drastically reduce any possible background.

## 4 Appendix

### 4.1 Cost estimates

The cost estimates for drilling pipes downstream of the Hall A beam dump are based on a budgetary bid for a single 16" pipe at location C indicated in Fig. ???. A cross section of the pipe (or "well") is shown in Fig. ???. The budgetary quote was adjusted by Suresh Chandra (JLab Facilities) to account for additional effort/work needed to complete the project. The resulting cost estimate is shown in Fig. ???. The following items were included in the cost:

- concrete slab on grade as a base for experimental test
- ground exploration in advance of drilling
- air blower to keep the well dry during test
- drilling of the hole proper; installing a pipe suitable for use as a guide for the detector apparatus
- backfill and compaction
- generator (on loan from facilities) to provide temporary power for one-week test (3KVA).

Based on the budgetary bid, two cost estimates were made for 10" pipes based on previous experience with such similar projects. The estimates are shown in Figs. ?? and ?? at locations B and C of Fig. ???. Given that the muon rate changes considerably with distance to the dump, we believe that two pipes are necessary to reliably understand the rate measurements. The estimated cost to drill two 10" pipes is \$40k. The typical time schedule for completing the project would be 8 weeks to prepare the contract, 6 weeks to award, and 6 weeks to complete the work, i.e. five months total.

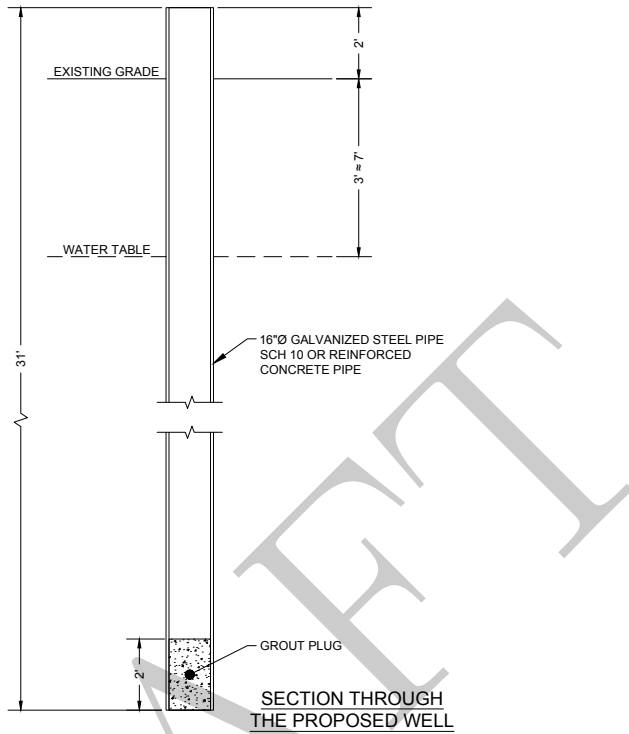
### 4.2 Work- & time-plan

The two wells will be drilled in locations **B** and **C** in the area downstream of Hall-A beam-dump as shown in Fig ?? inserting a 10" pipe as described in the previous Section. The test would require to run during the day, approximately for 4 calendar days (assuming 8h day shifts only and 50% efficiency of CEBAF to deliver  $10 \mu\text{A}$ , 11 GeV electron beam<sup>‡</sup> would correspond to less than 1 PAC days ) The detector will be lowered in the pipe and positioned at different depth measuring counting rates per each setting. Table ?? shows the expected CsI(Tl) rates and collected statistics. If possible we would like to do a beam current scan to check the expected count rate scaling. The beam-on status and the beam current are the only relevant accelerator information, accessible off-line by EPICS values stored in the database<sup>§</sup>. About 10 mn of stable beam ( $\frac{\Delta I_{Beam}}{I_{Beam}} < 10\%$ ) will be enough to assess the relationship between beam current and detected muon rate and establish a normalisation factor. If possible, we would like to perform a beam current scan to check the normalisation consistency. The scan would require 1h of dedicated beam-time coordinated with the Hall-A physics program to vary within a factor of 10 the beam current. It is worth mentioning, since the pipes will remain in place, it will be possible to plan in future other opportunistic measurements with different Hall-A beam current/energy set-ups.

---

<sup>‡</sup>As already noticed, this measurement is possible for beam currents ranging from 1 to  $100 \mu\text{A}$ .

<sup>§</sup>Synchronisation between BDX-Hodo DAQ and EPICS data is required at level of 1s.



Date:

1/27/17

**Cost Estimate for BDX Experiment - One 16" Well**

NUMBER	DESCRIPTION	QUANTITY	UNITS	RATE	AMOUNT	Sub's O&P	Contingency	Total
1	Well Installed 16" diameter - (Budgetary Bid + 5% for safety training & JLab work conditions)	1.00	Ea.	\$15,750	\$15,750		25%	\$19,688
2	Backfill & compaction	1.00	Ea.	\$3,000	\$3,000	25%	25%	\$4,688
3	Generator	1.00	Ea.	\$1,000	\$1,000	25%	25%	\$1,563
4	Concrete slab on grade 5'x5'x6" (To act also as Wt. against uplift)	1.00	Ea.	\$500	\$500	25%	25%	\$781
5	Ground exploration	1.00	Ea.	\$1,200	\$1,200	25%	25%	\$1,875
6	Air Blower to keep the well dry	1.00	Ea.	\$1,000	\$1,000	25%	25%	\$1,563
Grand Total								\$30,156

**NOTES:**

- 1) The Estimate is based on the assumption that **no radioactive contamination** of underground soil or water is encountered during drilling of the well.
- 2) Ground exploration will need to be done before detailed design done. This will also be used to ascertain no radioactive contamination in the well area.

Figure 23: Preliminary cost estimate for a single 16" pipe.

Date:

1/27/17

**Cost Estimate for BDX Experiment - One 10" Well**

NUMBER	DESCRIPTION	QUANTITY	UNITS	RATE	AMOUNT	Sub's O&P	Contingency	Total
1	Well Installed 10" diameter (Cost Based on bid for 16" well)	1.00	Ea.	\$12,000	\$12,000		25%	\$15,000
2	Backfill & compaction	1.00	Ea.	\$2,500	\$2,500	25%	25%	\$3,906
3	Generator	1.00	Ea.	\$1,000	\$1,000	25%	25%	\$1,563
4	Concrete slab on grade 5'x5'x6" (To act also as Wt. against uplift)	1.00	Ea.	\$500	\$500	25%	25%	\$781
5	Ground exploration	1.00	Ea.	\$1,200	\$1,200	25%	25%	\$1,875
6	Air Blower to keep the well dry	1.00	Ea.	\$1,000	\$1,000	25%	25%	\$1,563
Grand Total								\$24,688

**NOTES:**

- 1) The Estimate is based on the assumption that **no radioactive contamination** of underground soil or water is encountered during drilling of the well.
- 2) Ground exploration will need to be done before detailed design done. This will also be used to ascertain no radioactive contamination in the well area.

Figure 24: Preliminary cost estimate for a single 10" pipe.

Date:

1/27/17

**Cost Estimate for BDX Experiment - Two 10" Wells**

NUMBER	DESCRIPTION	QUANTITY	UNITS	RATE	AMOUNT	Sub's O&P	Contingency	Total
1	Well Installed 10" diameter (Cost Based on bid for 16" well)	2.00	Ea.	\$10,000	\$20,000		25%	\$25,000
2	Backfill & compaction	2.00	Ea.	\$2,000	\$4,000	25%	25%	\$6,250
3	Generator	1.00	Ea.	\$1,000	\$1,000	25%	25%	\$1,563
4	Concrete slab on grade 5'x5'x6" (To act also as Wt. against uplift)	2.00	Ea.	\$500	\$1,000	25%	25%	\$1,563
5	Ground exploration	1.00	Ea.	\$1,200	\$1,200	25%	25%	\$1,875
6	Air Blower to keep the well dry	2.00	Ea.	\$1,000	\$2,000	25%	25%	\$3,125
Grand Total								\$39,375

**NOTES:**

- 1) The Estimate is based on the assumption that **no radioactive contamination** of underground soil or water is encountered during drilling of the well.
- 2) Ground exploration will need to be done before detailed design done. This will also be used to ascertain no radioactive contamination in the well area.

Figure 25: Preliminary cost estimate for two 10" pipes.